Adiabatic response and quantum thermoelectrics for *ac* driven quantum systems

María Florencia Ludovico,[1,2] Francesca Battista,[1,2] Felix von Oppen,[3] and Liliana Arrachea[1,2]

[1] *Departamento de Física, FCEyN, Universidad de Buenos Aires and IFIBA, Pabellón I, Ciudad Universitaria, 1428 CABA Argentina*

[2] *International Center for Advanced Studies, UNSAM, Campus Miguelete, 25 de Mayo y Francia, 1650 Buenos Aires, Argentina*

[3] *Dahlem Center for Complex Quantum Systems and Fachbereich Physik, Freie Universität Berlin, 14195 Berlin, Germany*

We generalize the theory of thermoelectrics to include coherent electron systems under adiabatic *ac* driving, accounting for quantum pumping of charge and heat as well as the associated work exchange between electron system and driving potentials. We derive the relevant response coefficients in the adiabatic regime and show that they obey Onsager reciprocity relations. We analyze the consequences of our generalized thermoelectric framework for quantum motors, generators, heat engines, and heat pumps, characterizing them in terms of efficiencies and figures of merit.

PACS numbers: 73.23.-b, 72.10.Bg, 73.63.Kv, 44.10.+i

Introduction. Describing the relation between particle and energy currents is at the heart of thermoelectrics [1–5]. For *dc* driving with small temperature gradients and bias voltages, linear-response relations between the currents and the applied forces constitute the basis to describe thermoelectric phenomena. When combined with the basic principles of thermodynamics, the resulting theory has the beauty of simplicity and the strength of high predictive power. Specifically, it allows for a successful characterization of the efficiency of various thermoelectric machines in terms of the figure of merit introduced by Ioffe in 1949 [6].

An important challenge is to incorporate genuine quantum effects associated with coherent transport in nanodevices into this theoretical framework for thermoelectric effects. Here, we address how to include adiabatic quantum pumping as a paradigm of coherent-transport effects into a suitably generalized thermoelectric framework and explore the fundamental relations of the corresponding quantum machines. Quantum pumping generates nonzero *dc* currents by locally applying purely *ac* drivings to a quantum coherent conductor [7–9]. It generates both charge and energy currents [10] and enables heat pumping and the exchange of work between different driving forces [11, 12]. By combining adiabatic *ac* driving with the application of *dc* voltages it is also possible to exchange work between the *dc* electromotive forces and the *ac* ones [13]. Furthermore, by a suitable architecture of the device, part of the electrical work can be transformed into mechanical work, providing a basis for the operation of nanomotors and nanoengines [13–18]. The effect of *ac* driving to pump charge and heat against *dc* chemical potentials and temperature gradients was also investigated in arrays of quantum dots [19].

The aim of the present work is to extend linear-response theory to systems under adiabatic driving, including the energy flux between the electrons and the *ac* forces on equal footing with the heat and particle fluxes. This allows us to describe the operation of the generic two-terminal device sketched in Fig. 1 as a motor, generator (Fig. 1a), heat engine, or heat pump (Fig. 1b). Specifically, we derive generalized Osager relations and an appropriate figure of merit for this device which is driven by *ac* potentials in addition to gradients of chemical potential and temperature.

Adiabatic response. We begin by evaluating the currents and forces which are induced by a set of time-periodic parameters in the adiabatic approximation. We collect the parameters $V_i(t)$ of the Hamiltonian $\hat{\mathcal{H}}$ into a vector $\mathbf{V}(t) = \mathbf{V}(t+\mathcal{T}) = (V_1(t), V_2(t), \ldots)$ so that $\hat{\mathcal{H}} = \hat{\mathcal{H}}(\mathbf{V}(t))$, where $\mathcal{T} = 2\pi/\omega$ is the driving period. In the lowest order in the adiabatic approximation, the system is described by the frozen density matrix $\hat{\rho}_t$ for the Hamiltonian $\hat{\mathcal{H}}_t$ with t treated as a parameter. Accounting for the temporal variation of $\mathbf{V}(t)$ to lowest order, we can approximate the time evolution operator as $\hat{U}(t,t_0) \simeq \mathrm{T}\exp\{-i\hat{\mathcal{H}}_t(t-t_0) - i\int_{t_0}^{t} dt'(t-t')\hat{\mathbf{F}}\cdot\dot{\mathbf{V}}(t)\}$ in terms of the generalized force $\hat{\mathbf{F}}(t) = -\frac{\partial\hat{\mathcal{H}}(t)}{\partial\mathbf{V}(t)}$. To linear order in the small "velocity" $\dot{\mathbf{V}}(t)$, we can now follow the usual steps of linear response theory [20] and express the

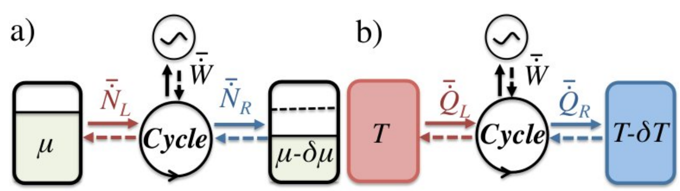

FIG. 1. Sketch of the setup. A coherent quantum conductor is driven by time-periodic potentials and connected to two reservoirs biased by (a) a chemical-potential difference $\delta\mu$ or (b) a temperature gradient δT, or both. Heat and charge are exchanged with the reservoirs and work is exchanged with the *ac* sources. The solid (dashed) lines indicate (a) the motor (generator) mode of the device, and (b) the heat engine (heat pump) modes.

expectation value $O(t)$ of an observable $\hat{O}$ at time t as

$$O(t) \simeq \langle \hat{O} \rangle_t - i \int_{t_0}^{t} dt'(t-t') \langle \left[\hat{O}(t), \hat{\mathbf{F}}(t') \right] \rangle_t \dot{\mathbf{V}}(t) = \langle \hat{O} \rangle_t + \mathbf{\Lambda}_t^{O\mathbf{F}} \cdot \dot{\mathbf{V}}(t). \quad (1)$$

Here, the operators $\hat{O}(t)$ and $\hat{\mathbf{F}}(t')$ are defined in the Heisenberg representation with respect to the frozen Hamiltonian $\mathcal{H}_t$ and $\langle \ldots \rangle_t$ denotes the expectation value with respect to the frozen density matrix $\hat{\rho}_t$, while $\mathbf{\Lambda}_t^{O\mathbf{F}}$ can be expressed through the retarded adiabatic susceptibility $\chi_t^{O,\mathbf{F}}(t-t') = -i\theta(t-t')\langle [\hat{O}(t), \hat{\mathbf{F}}(t')] \rangle_t$. We now expand the frozen average to linear order in an applied bias $\delta\mu$, yielding $\langle \hat{O} \rangle_t \simeq \Lambda_t^{Oc} \delta\mu$, where the linear-response coefficient Λ_t^{Oc} is given by the usual Kubo formula. Applying this procedure specifically to the charge current $J^c(t)$ and the forces $\mathbf{F}(t)$ (and postponing the heat currents and temperature gradients for further below), we obtain

$$\begin{pmatrix} J^c(t) \\ \mathbf{F}(t) \end{pmatrix} = \begin{pmatrix} J_t^c \\ \mathbf{F}_t \end{pmatrix} + \begin{pmatrix} \Lambda_t^{cc} & \mathbf{\Lambda}_t^{cf} \\ \mathbf{\Lambda}_t^{fc} & \hat{\mathbf{\Lambda}}_t^{ff} \end{pmatrix} \begin{pmatrix} \delta\mu \\ \dot{\mathbf{V}}(t) \end{pmatrix}, \quad (2)$$

to linear order in $\delta\mu$ and $\dot{\mathbf{V}}(t)$.

The terms in Eq. (2) have clear physical interpretations. The first term on the right hand side collects the currents and forces evaluated with the frozen density matrix $\hat{\rho}_t$ in equilibrium (i.e., for $\delta\mu = 0$). These terms have zero mean when averaged over one period of the *ac* fields. The forces can be thought of as conservative Born-Oppenheimer forces and expressed as a gradient of the equilibrium energy of the system with respect to $\mathbf{V}(t)$. For several potentials this term may lead to exchange of work between the different forces F_j without dissipation. Such processes were considered in Refs. 11 and 12. Adiabatic quantum pumping of charge by the *ac* potentials is described by $\mathbf{\Lambda}_t^{cf}$, while $\mathbf{\Lambda}_t^{fc}$ captures the modification of the forces by the applied bias $\delta\mu$. Both contributions are generally nonzero when averaged over a period, implying that this contribution to the force is *non*conservative. This was discussed for non-interacting electrons coupled to adiabatic nanomechanical systems [21, 22] and nanomagnets [23], where in the latter case it corresponds to the spin-transfer torque. The diagonal components describe the usual conductivity through Λ_t^{cc} and the velocity-dependent force through $\hat{\mathbf{\Lambda}}_t^{ff}$. In time-reversal symmetric systems, the latter is symmetric and describes a frictional force. Without time-reversal symmetry, $\hat{\mathbf{\Lambda}}_t^{ff}$ may have an antisymmetric part which is analogous to the Lorenz force [22].

Equation (2) has an important consequence. The coefficients are related to susceptibilities evaluated with the frozen equilibrium state ρ_t. Thus, we can apply arguments based on the microreversibility of time-independent Hamiltonians and consequently, the response coefficients Λ_t^{ij} satisfy the generalized Onsager relations (see the Supplementary Material 1 for details)

$$\Lambda_t^{cc}(B) = \Lambda_t^{cc}(-B) \quad , \quad \hat{\mathbf{\Lambda}}_{ij}^{ff}(B) = s_i s_j \hat{\mathbf{\Lambda}}_{ji}^{ff}(-B)$$
$$\mathbf{\Lambda}_j^{cf}(B) = s_j \mathbf{\Lambda}_j^{fc}(-B), \quad (3)$$

where $s_j = \pm 1$ depending on the parity of the operators $\hat{F}_j$ under time reversal. Similar relations were found for closed systems [24]. The second line imposes a relation between the adiabatic quantum pumping of charge and the nonconservative force. This relation was previously found for noninteracting adiabatic quantum motors at zero-temperature and $B = 0$ [13]. Eqs. (3) are valid at finite T and in the presence of many-body interactions.

Generalized thermoelectric framework. Thermoelectrics considers particle and heat currents in response to chemical-potential and temperature differences. In the presence of *ac* driving as in the devices in Fig. 1, we have to include the quantum pumping of particles and heat as well as the work performed by or on the *ac* potentials on the same footing. To develop the corresponding quantum thermoelectrics, we first consider the entropy production of the system. After averaging over one period of the ac driving, the net dissipation occurs only in the electrodes and we can write

$$\overline{\dot{S}} = \frac{\overline{\dot{Q}_L}}{T_L} + \frac{\overline{\dot{Q}_R}}{T_R}, \quad (4)$$

where the average heat flux in lead α is given by $\overline{\dot{Q}}_\alpha = \overline{\dot{E}}_\alpha - \mu_\alpha \overline{\dot{N}}_\alpha$. The energies E_α and particle numbers N_α satisfy the conservation laws

$$\overline{\dot{N}}_R = -\overline{\dot{N}}_L, \qquad \overline{\dot{E}}_L + \overline{\dot{E}}_R = \overline{\dot{W}}. \quad (5)$$

While particle-number conservation takes the same form as in standard thermoelectrics, energy conservation must account for the additional work W performed by the *ac* potentials on the electron system. The corresponding power can be expressed as $\dot{W} = -\sum_j F_j(t)\dot{V}_j(t)$, yielding the entropy production

$$\overline{\dot{S}} = \overline{\dot{N}}_R \frac{\delta\mu}{T} + \overline{\dot{Q}}_R \frac{\delta T}{T^2} - \sum_j \overline{F_j(t) \frac{\dot{V}_j(t)}{T}} \quad (6)$$

to linear oder in the applied bias $\delta\mu = \mu_L - \mu_R$ and temperature difference $\delta T = T_L - T_R$. Note that after averaging over a period, the conservative Born-Oppenheimer forces in Eq. (2) do not contribute to entropy production. Then, the power can be expressed in linear response and for $\delta T = 0$ as

$$\overline{\dot{W}} = -\sum_j \overline{(\hat{\mathbf{\Lambda}}_t^{fc})_j \dot{V}_j(t)} \delta\mu + \sum_{j,l} \overline{(\hat{\mathbf{\Lambda}}_t^{ff})_{jl} \dot{V}_j(t) \dot{V}_l(t)}. \quad (7)$$

Here, the first term on the right-hand side describes the work performed by the nonconservative force originating from the applied voltage $\delta\mu$ (δT would contribute a similar term) and the second term is the dissipated power due to a frictional force on the *ac* potentials.

In conventional thermoelectrics, one now defines the particle and heat fluxes $J_1 = \overline{\dot{N}}_R$ and $J_2 = \overline{\dot{Q}}_R$ as well as the associated affinities $X_1 = \delta\mu/T$ and $X_2 = \delta T/T^2$ [28, 29]. To extend thermoelectrics to the present situation, we need to identify appropriate fluxes and affinities for the *ac* driving terms.

At first sight, Eq. (6) may suggest to define the $-F_j$ as fluxes and the $\dot{V}_j/T$ as the associated affinities. However, Eq. (6) holds only after averaging over one period. Before time averaging, the conservation laws involve additional terms [25] and the forces $F_j(t)$ contain contributions that are conservative. We can identify an appropriate affinity by noting that after averaging, the first term in Eq. (7) is proportional to ω, while the second term is proportional to ω^2. It is thus natural to define the affinity $X_3 = \hbar\omega/T$ with associated flux $J_3 = \overline{\dot{W}}/(\hbar\omega)$ [28, 29]. This yields

$$\overline{\dot{S}} = \sum_j J_j X_j. \tag{8}$$

for the rate of entropy production. We complete our quantum thermoelectrics scheme by linear-response relations between fluxes and affinities,

$$J_i = \sum_k L_{ik} X_k. \tag{9}$$

The linear-response coefficients L_{ij} can be readily related to the coefficients which appeared in Eq. (2). Explicit expressions – in terms of Green functions [11, 26, 27] or scattering matrices [10] and valid for noninteracting systems – can be found in the Suplementary Material 2.

Clearly, the coefficients L_{ij} also satisfy Onsager relations, namely

$$L_{ii}(B) = L_{ii}(-B) \ \ , \ \ L_{ij}(B) = \pm L_{ji}(-B), \tag{10}$$

with $i \neq j$. Time-reversal symmetry (which is assumed from now on) thus implies $L_{12} = L_{21}$, but $L_{13} = -L_{31}$ and $L_{23} = -L_{32}$. We will see that this has important consequences for the definition of figures of merit.

Motors and generators. First consider a situation with applied *ac* driving forces and *dc* bias $\delta\mu$, but uniform temperature T. Then, the device in Fig. 1(a) can operate as a quantum motor or generator. When the *ac* potentials pump particles into the reservoir with lower chemical potential, the gain in electrical energy can be used to perform work on the source of the *ac* potentials. This occurs for $L_{31}\delta\mu/T < 0$ and corresponds to a motor as the work performed on the *ac* potentials can be further transformed, say, into mechanical work [13]. When reversing the sign of $\delta\mu$ and thus $L_{31}\delta\mu/T > 0$, the *ac* potentials pump particles into the reservoir with higher chemical potential and we have a generator.

Using $X_2 = 0$, the rate of entropy production becomes

$$\overline{\dot{S}} = L_{11}X_1^2 + L_{33}X_3^2 + (L_{13} + L_{31})\, X_1 X_3. \tag{11}$$

Interestingly, the last term on the right-hand side vanishes due to the Onsager symmetries, and L_{13} as well as L_{31} do not affect the entropy production. As a consequence, the second law of thermodynamics imposes $L_{11} > 0$ and $L_{33} > 0$. This should be contrasted with the usual thermoelectric case, where the second law imposes $\det L = L_{11}L_{22} - L_{12}^2 > 0$ in addition.

We are now ready to characterize the performance of adiabatically-driven quantum motors or generators in terms of efficiencies and figures of merit. The efficiency $\eta^{\rm mot}$ of a motor is measured by the ratio of the work per unit time $-\overline{\dot{W}}$ performed on the *ac* potentials and the power TJ_1X_1 injected by the voltage source. Similarly, the efficiency of the generator $\eta^{\rm gen}$ is given by the inverse of this ratio,

$$\eta^{\rm mot} = \frac{1}{\eta^{\rm gen}} = -\frac{X_3 J_3}{X_1 J_1}. \tag{12}$$

These efficiencies are restricted by the second law of thermodynamics, as discussed in the Supplementary Material 3.

Inserting the linear-response relation (9) and maximizing this expression as a function of, say, X_1 at fixed X_3, we find the maximal efficiency

$$\eta^{\rm max} = \frac{\sqrt{1+\zeta} - 1}{\sqrt{1+\zeta} + 1} \tag{13}$$

and identified the figure of merit

$$\zeta = \frac{-L_{13}L_{31}}{L_{11}L_{33}}. \tag{14}$$

These results for $\eta^{\rm max}$ and ζ are valid for both motors and generators.

Equations (13) and (14) should be contrasted with conventional thermoelectrics [2–6], where the optimal efficiency satisfies an analogous expression, with the Carnot efficiency as an additional factor and the figure of merit replaced by the familiar value $ZT = L_{12}^2/\det L$. The absence of the Carnot efficiency in Eq. (13) reflects that electrical energy can be fully converted into other forms of energy so that $\eta^{\rm mot}$ is only bounded by one. This limit is reached when $\zeta \to \infty$, i.e., when one of the dissipative coefficients L_{11} or L_{33} approaches zero. The different form of the figure of merit can be traced back to the fact that L_{13} and L_{31} do not affect the entropy production.

Heat engine and heat pump. Analogous results are obtained when the device is driven by a temperature gradient δT at constant chemical potential ($X_1 = 0$), cf. Fig. 1(b). When the device operates as a heat engine, i.e., for $L_{32}\delta T/T^2 < 0$, heat flows to the cold reservoir and the system performs work on the *ac* potentials. Conversely, the device operates as a heat pump when $L_{32}\delta T/T^2 > 0$, where heat is pumped to the hot reservoir by the *ac* potentials.

As a result of the Onsager symmetry $L_{23} = -L_{32}$, we again find that the second law imposes $L_{22} > 0$ and $L_{33} > 0$. Characterizing the efficiency of heat engine and heat pump through

$$\eta^{\rm he} = \frac{1}{\eta^{\rm hp}} = -\frac{X_3 J_3}{X_2 J_2}, \tag{15}$$

and maximizing the efficiency as before, we find

$$\eta^{\rm max} = \eta_c \frac{\sqrt{1+\tilde{\zeta}}-1}{\sqrt{1+\tilde{\zeta}}+1} \tag{16}$$

with the figure of merit

$$\tilde{\zeta} = \frac{-L_{23}L_{32}}{L_{22}L_{33}}. \tag{17}$$

As this device converts between heat and mechanical energy, the efficiency is bounded by the Carnot efficiency $\eta_c = \delta T/T$ for the heat engine or $\eta_c = T/\delta T$ for the heat pump, as it should be.

Application to model system. To illustrate these concepts, we consider a quantum dot with a single level coupled to two reservoirs [Fig. 2(a)]. We assume that the dot level and the barriers can be modulated periodically in time by *ac* gate potentials $V_j(t) = V_j^0 \cos(\omega t + \delta_j)$ (with $j = 1, 3$ corresponding to the barriers and $j = 2$ to the dot level). This model can describe a single-electron source, similar to the GHz pump realized experimentally in Ref. 30. Here, we focus on the results. Calculations are provided in the Supplementary Material 2.

For definiteness, we consider an applied bias $\delta\mu$ at $T = 0$, i.e., the motor/generator regime. In Fig. 2(b), we plot the transport coefficients and the maximum efficiency $\eta^{\rm max}$ as functions of the chemical potential μ of the left reservoir. Large values of the figure of merit require a large charge pumping coefficient L_{13} along with a small value of $L_{33}L_{11}$, *i.e.*, low friction or conductance. In the absence of driving at the central dot ($V_2(t) = 0$) the conductance peaks near $L_{11} = 1$ when μ is in resonance with the dot level. Driving the dot level with a phase lag relative to the barrier oscillations ($\delta_2 - \delta_i \neq 0$ for $i = 1, 3$) favors charge pumping and decreases the conductance by dynamically tuning the dot off resonance. In this way, high efficiencies can be achieved despite large values of L_{33}.

As the chemical potential passes the dot level, the pumping coefficient changes sign, and the system switches from motor mode [$L_{31}\delta\mu/T < 0$; see region M in the Fig. 2 (b)] to generator mode [$L_{31}\delta\mu/T > 0$, see region G in the Fig. 2(b)]. The efficiency becomes minimal when the chemical potential is resonant with the dot level, where the conductance is maximal and pumping vanishes by particle-hole symmetry.

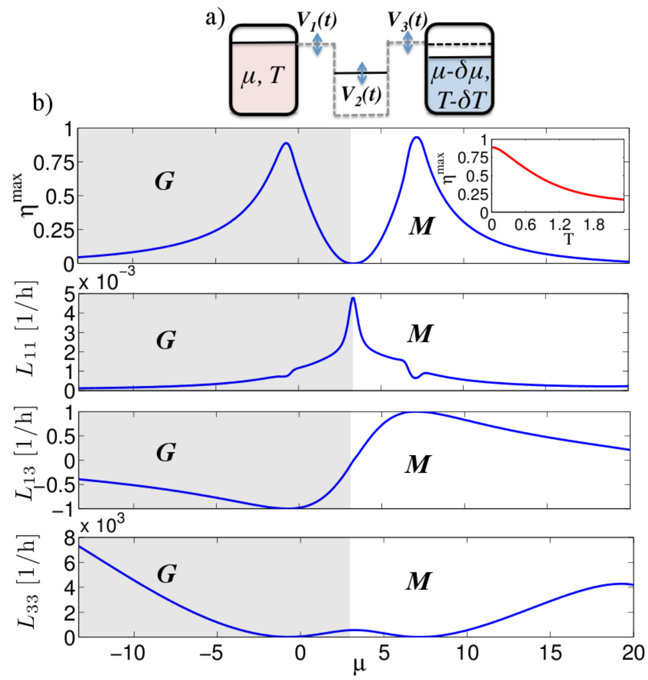

FIG. 2. (a) Sketch of the device. A single-level quantum dot ($j = 2$) and its tunnel barriers ($j = 1, 3$) represented by a discrete model with local energies $\varepsilon_1 = \varepsilon_3 = 3.3$ and $\varepsilon_2 = -1$, are driven by periodic gate potentials $V_j(t) = V_j^0 \cos(\omega t + \delta_j)$, with $V_1^0 = V_3^0 = 4$, $V_2^0 = 23$, $\delta_1 = 0$, $\delta_2 = \pi/2$, and $\delta_3 = \pi$. The tunneling amplitudes between barriers and dot are $w = 1$ and $w_L = w_R = 0.7$ between barriers and reservoirs. The latter have $\mu_L = \mu$, $\mu_R = \mu - \delta\mu$ and temperature T. (b) Maximum efficiency $\eta^{\rm max}$ and transport coefficients at $T = 0$ for the motor (M) or generator (G) modes. Inset: $\eta^{\rm max}$ for generator/motor with $\mu = -0.7$ ($\mu = 7.2$).

The device can also operate as a heat engine or pump when imposing a temperature gradient. As this requires finite T, quantum effects are less pronounced and efficiencies lower than those shown in Fig. 2. However, we find that for appropriate parameters these may still be as high as $\approx 0.4\eta_c$.

Conclusions. Motivated in part by Jarzynski's equality [31] and Crook's theorem [32], there has recently been much interest in quantum thermodynamics, including fluctuation relations, work fluctuations, and the thermodynamic description of strongly coupled systems [33–35]. Here, we have provided a generalized thermoelectric framework to analyze the thermodynamics of *ac*-driven nanoscale systems which explicitly accounts for the effects of quantum pumping and the associated nonconservative forces. The latter enter the theory through an additional flux and affinity which we identify. We have derived the associated generalized Onsager relations, defined appropriate efficiencies and figures of merit for quantum motors, generators, heat engines, and heat pumps, and illustrated our results for a simple quantum-pump device.

Acknowledgments. We acknowledge useful discussions with A. Bruch, R. Bustos-Marun, S. Kusminskiy, and A. Nitzan. This work was supported by the Alexander-von-Humboldt Stiftung (L.A. and F.v.O.), CONICET (M.F.L. and F.B.), MINCyT and UBACyT (L.A.), as well as the Deutsche Forschungsgemeinschaft (F.v.O.).

[1] L. Onsager, Phys. Rev. **38**, 2265 (1931); M. Büttiker, Phys. Rev. Lett. **57**, 1761 (1986); P. N. Butcher, J. Phys.: Condens. Matter **2**, 4869 (1990).
[2] G. Benenti, G. Casati, T. Prosen, K. Saito, arXiv:1311.4430.
[3] G. Benenti, K. Saito, and G. Casati, Phys. Rev. Lett. **106**, 230602 (2011).
[4] K. Brandner, K. Saito, and U. Seifert, Phys. Rev. Lett. **110**, 070603 (2013).
[5] O. Entin-Wohlman, Y. Imry, and A. Aharony, Phys. Rev. B **91**, 054302 (2015).
[6] M. V. Vedernikov and E. K. Iordanishvili, 17th Int. Conf. on Thermoelectrics vol 1, pp. 37-42 (1998)
[7] D. J. Thouless, Phys. Rev. B **27**, 6083 (1983).
[8] M. Büttiker, H. Thomas, and A. Prêtre, Z. Phys. B **94**, 133 (1994).
[9] P.W. Brouwer, Phys. Rev. B **58**, 10135(R) (1998).
[10] M. Moskalets and M. Büttiker, Phys. Rev. B **69**, 205316 (2004).
[11] L. Arrachea, M. Moskalets, and L. Martin-Moreno, Phys. Rev. B **75**, 245420 (2007).
[12] M. Moskalets and M. Büttiker, Phys. Rev. B **80**, 081302(R) (2009).
[13] R. Bustos-Marun, G. Refael and F. von Oppen, Phys. Rev. Lett. **111**, 060802 (2013).
[14] A. M. Fennimore, T. D. Yuzvinsky, W. Q. Han, M. S. Fuhrer, J. Cumings, and A. Zettl, Nature **58**, 408410, (2003).
[15] A. del Campo, J. Goold, and M. Paternostro, Scientific Reports **4**, 6208 (2014).
[16] F. Mazza, R. Bosisio, G. Benenti, V. Giovannetti, R. Fazio, and F. Taddei, New J. Phys. **16**, 085001 (2014).
[17] T. E. Humphrey, R. Newbury, R. P. Taylor, and H. Linke, Phys. Rev. Lett. **89**, 116801 (2002).
[18] T. E. Humphrey and H. Linke, Phys. Rev. Lett. **94**, 096601 (2005).
[19] S. Juergens, F. Haupt, M. Moskalets, and J. Splettstoesser, Phys. Rev. B **87**, 245423 (2013).
[20] H. Bruus and K. Flensberg, *Many-body quantum field theory in condensed matter physics*, (Oxford, 2005).
[21] J. T. Lu, M. Brandbyge, and P. Hedegard, Nano Lett. **10**, 1657 (2010).
[22] N. Bode, S. Viola Kusminskiy, R. Egger, and F. von Oppen, Phys. Rev. Lett. **107**, 036804 (2011).
[23] N. Bode, L. Arrachea, G. S. Lozano, T. S. Nunner, and F. von Oppen, Phys. Rev. B 85, 115440 (2012) .
[24] D. Cohen, PRB **68**, 155303 (2003).
[25] M. F. Ludovico, J. S. Lim, M. Moskalets, L. Arrachea and D. Sanchez, Phys. Rev. B **89**, 161306(R) (2014).
[26] L. Arrachea and M. Moskalets, Phys. Rev. B **74**, 245322 (2006).
[27] M. F. Ludovico and L. Arrachea, Phys. Rev. B **87**, 115408 (2013).
[28] H. Callen, Phys. Rev. **73**, 1349 (1948).
[29] L. D. Landau and E. M. Lifshitz, Statistical Physics, Vol.5, Pergamon press, London-Paris (1959).
[30] M. D. Blumenthal, B. Kaestner, L. Li, S. Giblin, T. J. B. M. Janssen, M. Pepper, D. Anderson, G. Jones, and D. A. Ritchie, Nature Phys. **3**, 343 (2007).
[31] C. Jarzynski, Phys. Rev. Lett. **78**, 2690 (1997).
[32] G. E. Crooks, Phys. Rev. E **60**, 2721 (1999).
[33] J. Kurchan, J. Stat. Mech. P07005 (2007).
[34] M. Esposito, U. Harbola and S. Mukamel, Rev. Mod. Phys. **81**, 1665 (2009).
[35] M. Campisi, P. Hänggi and P. Talkner, Rev. Mod. Phys. **83**, 771 (2011).

SUPLEMENTARY MATERIAL

1. ONSAGER COEFFICIENTS AND RECIPROCITY RELATIONS

Quite generally the Hamiltonian of the system can be expressed as follows

$$\hat{\mathcal{H}}(\mathbf{V}(\mathbf{t})) = \hat{\mathcal{H}}_0 - \sum_j \hat{F}_j V_j(t), \tag{18}$$

where $\mathcal{H}_0$ is the time-independent part of the Hamiltonian and F_j are hermitian operators. The matrix elements entering $\mathbf{\Lambda}_t^{cf}$ read

$$\Lambda_j^{cf} = -i\int_{-\infty}^{\infty} dt'(t-t')\theta(t-t')\langle\Big[\hat{J}^c(t), \hat{F}_j(t')\Big]\rangle_t \equiv \int_{-\infty}^{\infty} d\tau\tau\chi_t^{J,F_j}(\tau), \tag{19}$$

where we have defined the retarded susceptibility $\chi_t^{J,F_j}(\tau) = -i\theta(\tau)\langle\Big[\hat{J}^c(\tau), \hat{F}_j(0)\Big]\rangle_t$. In the latter step we have stressed the fact that, for evolutions with the operator $U(\tau) = e^{-i\tau\hat{H}_t}$, being $\hat{H}_t = \hat{H}\left(\mathbf{V}(t)\right)$ the frozen Hamiltonian, the actual time argument of the integrand of (19) is $\tau = t - t'$. Representing the susceptibility in terms of the Fourier transform we can also write the previous expression as

$$\Lambda_j^{cf} = \mathrm{Re}\left[\int_{-\infty}^{+\infty} d\tau \int_{-\infty}^{+\infty} \frac{d\omega}{2\pi i} e^{-i\omega\tau}\partial_\omega\chi_t^{J,F_j}(\omega)\right] = \mathrm{Re}\left[-i\int_{-\infty}^{+\infty} d\omega\partial_\omega\chi_t^{J,F_j}(\omega)\delta(\omega)\right] = \lim_{\omega\to 0}\frac{\mathrm{Im}\left[\chi_t^{J,F_j}(\omega)\right]}{\omega}, \tag{20}$$

where we have used that the spectral function $\mathrm{Im}\left[\chi_t^{J,F_j}(\omega)\right]$ is odd in ω, hence $\mathrm{Im}\left[\chi_t^{J,F_j}(\omega)\right] = 0$ [20].

Analogously, the matrix elements of $\hat{\Lambda}_t^{ff}$ can be written as

$$\begin{aligned}\Lambda_{ij}^{ff} &= -i\int_{-\infty}^{\infty} dt'(t-t')\theta(t-t')\langle\Big[\hat{F}_i(t), \hat{F}_j(t')\Big]\rangle_t = \mathrm{Re}\left[-i\int_{-\infty}^{+\infty} d\omega\partial_\omega\chi_t^{F_i,F_j}(\omega)\delta(\omega)\right] \\ &= \lim_{\omega\to 0}\frac{\mathrm{Im}\left[\chi_t^{F_i,F_j}(\omega)\right]}{\omega},\end{aligned} \tag{21}$$

where $\chi_t^{F_i,F_j}(\omega)$ is the Fourier transform of $\chi_t^{F_i,F_j}(\tau) = -i\theta(\tau)\langle\Big[\hat{F}_i(\tau), \hat{F}_j(0)\Big]\rangle_t$.

The calculation of the conductivity follows the usual procedure of the Kubo formula presented in text books [20]. We start by considering an extra perturbation due to the coupling to an electric field $E(t) = \partial_t A(t)$. In the Fourier domain the extra perturbation is $\mathcal{H}'(\omega) = \mathcal{J}\cdot E(\omega)/(i\omega)$, which leads to the definition of the dc conductance

$$\Lambda^{cc} = \lim_{\omega\to 0}\frac{\mathrm{Im}\left[\chi_t^{J,J}(\omega)\right]}{\omega}, \tag{22}$$

where $\chi_t^{J,J}(\omega)$ is the Fourier transform of $\chi_t^{J,J}(\tau) = -i\theta(\tau)\langle\Big[\hat{J}(\tau), \hat{J}(0)\Big]\rangle_t$.

Similarly, by evaluating the forces in linear response with respect to $\delta\mu$ leads to

$$\Lambda_j^{fc} = \lim_{\omega\to 0}\frac{\mathrm{Im}\left[\chi_t^{F_j,J}(\omega)\right]}{\omega}, \tag{23}$$

where $\chi_t^{F_j,J}(\omega)$ is the Fourier transform of $\chi_t^{F_j,J}(\tau) = -i\theta(\tau)\langle\Big[\hat{F}_j(\tau), \hat{J}(0)\Big]\rangle_t$.

The above definitions indicate that the susceptibilities $\chi_t^{O_i,O_j}$, with $\hat{O}_i$ a generic operator, satisfy microreversibility with respect to τ. It can be directly verified that $\chi_t^{O_i,O_j}(-\tau) = -i\theta(-\tau)\langle\Big[\hat{O}_i(-\tau), \hat{O}_j(0)\Big]\rangle_t = i\theta(-\tau)\langle\Big[\hat{O}_j(\tau), \hat{O}_i(0)\Big]\rangle_t = -i\theta(-\tau)\int_{-\infty}^{+\infty} d\omega/(\pi)\mathrm{Im}[\chi_t^{O_j,O_i}(\omega)]e^{-i\omega\tau}$. Hence, under a transformation $\tau \to -\tau$ the coefficient Λ_{ij} transforms to

$$\Lambda_{ij}^{O_i,O_j} \to_{\tau\to-\tau} \mathrm{Re}\left[i\int_{-\infty}^{+\infty}\frac{d\omega}{\pi}\mathrm{Im}[\chi_t^{O_j,O_i}(\omega)]\int_{-\infty}^{+\infty} d\tau\tau\theta(-\tau)e^{-i\omega\tau}\right] = \lim_{\omega\to 0}\frac{\mathrm{Im}\left[\chi_t^{O_j,O_i}(\omega)\right]}{\omega} = \Lambda_{ji}^{O_j,O_i}. \tag{24}$$

In the last step we have used $\int_{-\infty}^{0} d\tau \tau e^{-i\omega\tau} = \frac{1}{\omega^2} + i\pi\delta'(\omega)$.

In the presence of a magnetic field B, a time-reversal transformation implies changing $B \to -B$ in the Hamiltonian $\mathcal{H}_t$ defining the frozen density matrix $\hat{\rho}_t$ used to evaluate the expectation values. This property leads to the following Onsager relations for the usual susceptibilities in the presence of B, $\chi_t^{O_i,O_j}(B,\omega) = s_i s_j \chi_t^{O_j,O_i}(-B,\omega)$, where the signs $s_i, s_j = \pm$ depend on the parity of the operators $\hat{O}_i,\ \hat{O}_j$ under a time-reversal transformation. Therefore, taking into account (24), we see that the coefficients Λ_{ij}^{ff} satisfy the following general Onsager reciprocal relations

$$\Lambda_{ij}^{ff}(B) = s_i s_j \Lambda_{ji}^{ff}(-B), \tag{25}$$

where $s_i, s_j = \pm$ depending on the parity under $B \to -B$ of the operators $\hat{F}_i(B),\ \hat{F}_j(B)$. Using exactly the same arguments we can prove

$$\Lambda_j^{cf}(B) = s_j \Lambda_j^{fc}(-B) \tag{26}$$

The case $s_j = 1$ is usual in density-like operators as in the example considered in the Supplementary Material 2, while $s_j = -1$ is usual in current operators like in the case of driving with time-dependent magnetic fields.

2. TWO-TERMINAL SETUP WITHOUT MANY-BODY INTERACTIONS

As mentioned before, the transport coefficients L_{ij} can be directly calculated from the coefficients Λ, which are in turn evaluated from the susceptibilities $\chi_t(\omega)$. Another possibility is to directly start from the expressions for the charge (32), heat (33) and work (35) currents, perform expansions in $\hbar\omega$, $\delta\mu$ and δT and identify from there the coefficients L. In the case of systems without many-body interactions this procedure is rather straightforward. In this section we present the ensuing results obtained when the currents are evaluated by recourse to Green's functions and Scattering Matrix formalisms as in Refs. 10 and 11. We will focus on the case $B = 0$.

Model

We start by considering a simple non-interacting model for the generic setup of Fig. 1. The central piece is connected to the two electron reservoirs, with chemical potentials μ_α and temperatures T_α, $\alpha = L, R$. It is also driven by an external time-dependent potential characterized by a set of time periodic parameters $V(t) \equiv (V_1(t), \dots, V_N(t))$ oscillating with a frequency ω. The Hamiltonian of the full system reads:

$$\hat{\mathcal{H}}(t) = \hat{\mathcal{H}}_c(t) + \hat{\mathcal{H}}_{res} + \hat{\mathcal{H}}_T. \tag{27}$$

The first term corresponds to the central driven conductor, which is described by a discrete model with N sites with local energies ε_m at which the ac potentials are applied, which are connected by tunneling amplitudes w

$$\hat{\mathcal{H}}_c(t) = \sum_{m=1}^{N} \left[(\varepsilon_m + V_m(t))\, d_m^\dagger d_m + \sum_{m=1}^{N-1} w\ d_m^\dagger d_{m+1} \right] + \text{h.c.} \tag{28}$$

The reservoirs are represented by Hamiltonians for free electrons with many degrees of freedom,

$$\hat{\mathcal{H}}_{res} = \sum_{\alpha=L,R,k_\alpha} E_{k_\alpha} c_{k_\alpha}^\dagger c_{k_\alpha}. \tag{29}$$

The Hamiltonian $\hat{\mathcal{H}}_T$ represents the tunneling between the reservoirs and the central system,

$$\hat{\mathcal{H}}_T = -\sum_{\alpha,k_\alpha,n} [w_\alpha d_{n_\alpha}^\dagger c_{k_\alpha} + h.c], \tag{30}$$

where n_α is the site of the central structure which is in contact to the reservoir α. In the example of Fig. 2 we consider precisely the Hamiltonian $\hat{\mathcal{H}}_c(t)$, which $N = 3$, where two barriers ($m = 1, 3$) and a quantum dot ($m = 2$) with diagonal energies $\varepsilon_m,\ m = 1, 2, 3$ are driven by three time-dependent gate voltages of the form $V_m(t) = V_m^0 \cos(\omega t + \delta_m)$.

In Ref. 11 it was shown that the averaged charge $\overline{\dot{N}}_\alpha$ and heat $\overline{\dot{Q}}_\alpha$ currents entering the reservoir α, as well as the mean power $\overline{\dot{W}}$ developed by the ac forces can be written in terms of the retarded Green function of the central structure connected to the reservoirs expanded in the Floquet-Fourier transform as

$$\hat{G^R}(t,t') = \sum_{n=-\infty}^{\infty} e^{-in\omega t} \int_{-\infty}^{\infty} \frac{dE}{2\pi} e^{-i\frac{E}{\hbar}(t-t')} \hat{\mathcal{G}}(n,E) \tag{31}$$

This function is calculated from the Hamiltonian $\hat{\mathcal{H}}(t)$ by solving the Dyson equation (see Refs. 11 and 26).

The resulting expression for the charge current is

$$\overline{\dot{N}}_\alpha = \frac{e}{h} \int dE \sum_{n,\beta} \left[f_\beta(E) - f_\alpha(E+n\hbar\omega)\right] |\hat{\mathcal{G}}_{\alpha\beta}(n,E)|^2 \hat{\Gamma}_\beta \hat{\Gamma}_\alpha. \tag{32}$$

The heat current reads

$$\overline{\dot{Q}}_\alpha = \overline{\dot{E}}_\alpha - \mu_\alpha \frac{\overline{\dot{N}}_\alpha}{e}, \tag{33}$$

with

$$\overline{\dot{E}}_\alpha = \frac{1}{h} \int_{-\infty}^{+\infty} dE \sum_n E[f_\beta(E) - f_\alpha(E+n\hbar\omega)] |\hat{\mathcal{G}}_{\alpha\beta}(n,E)|^2 \hat{\Gamma}_\beta \hat{\Gamma}_\alpha. \tag{34}$$

Similarly, the work performed by the *ac* potentials can be written as

$$\overline{\dot{W}} = -\frac{1}{h} \sum_{\alpha,l,n} \int_{-\infty}^{+\infty} dE \, n\hbar\omega f_\alpha(E) \mathrm{Im}\{\mathrm{Tr}\left[\hat{V}(n)\hat{\mathcal{G}}(n+l,E)\hat{\Gamma}_\alpha \hat{\mathcal{G}}^\dagger(l,E)\right]\}, \tag{35}$$

where $\hat{V}(n)$ are the Fourier components of $\hat{V}(t) = \sum_n \hat{V}(n) e^{in\omega t}$, being $\hat{V}(t)$ a matrix with diagonal elements $V_m(t)$. In the above expressions we introduced the hybridization matrix $\hat{\Gamma}_\alpha$ has a single element at the contact with the reservoir equal to $|w_\alpha|^2 2\pi \sum_{k_\alpha} \delta(E - E_{k_\alpha})$. For practical uses it can be considered in the wide band limit, thus, independent of E. The Fermi-Dirac distribution $f_\alpha(E) = [1 + e^{(E-\mu_\alpha)/T_\alpha}]^{-1}$ characterizes the thermal occupation of the electrons in the reservoirs (from now on we set the Boltzmann constant $k_B = 1$).

In what follows will consider only terms of the currents $J_1 = \overline{\dot{N}}_R$, $J_2 = \overline{\dot{Q}}_R$ and $J_3 = \overline{\dot{W}}/(\hbar\omega)$ upto $\mathcal{O}(\hbar\omega)$. These can be calculated using an alternative procedure which does not rely on the Floquet decomposition (see Refs 22 and 23). However, we prefer to start from (31) here because this representation stresses that $\hbar\omega$ appears in the arguments of the Fermi functions entering the integrands for the currents on the same footing as the chemical potential μ, which suggests that it makes sense to identify $\hbar\omega/T$ as an affinity.

The other possible approach is the Floquet scattering matrix formalism used in [10]. The elements $s_{ij}(E_m, E_n)$ of the Floquet scattering matrix $\hat{s}(E)$, with $E_n = E + n\hbar\omega$, are the amplitudes for an electron to scatter from lead j to lead i after acquiring $m - n$ Floquet quanta $\hbar\omega$. The general relation between the Floquet scattering matrix elements and the Fourier coefficients for the Green's function is the generalized Fisher-Lee formula [26]

$$s_{ij}(E_m, E_n) = \delta_{ij}\delta_{mn} - i\sqrt{\Gamma_i \Gamma_j} \mathcal{G}_{ij}(m-n, E_n). \tag{36}$$

Linear response

In order to calculate the currents J_l, $l = 1, 2, 3$ up to linear orders in $\hbar\omega$, $\delta\mu$ and δT we perform the following expansion of the Fermi function entering the integrands of Eqs. (32), (33) and (35)

$$f_\alpha(E+n\hbar\omega) \sim f_\alpha(E) + n\hbar\omega \partial_E f_\alpha(E) - \frac{\partial f(E)}{\partial E}(\mu_\alpha - \mu) - \frac{\partial f(E)}{\partial E} \frac{(E-\mu)}{T}(T_\alpha - T). \tag{37}$$

We also need to evaluate $\mathcal{G}(n.E)$ upto linear order in ω. This can be done by expanding the Dyson equation in powers of ω (see [25, 27]). Up to the first order in ω it reads

$$\hat{G}(t,E) \sim \hat{G^f}(t,E) + \hat{G^{(1)}}(t,E), \tag{38}$$

with $\hat{G}(t,E)=\sum_{n=-\infty}^{\infty}\hat{\mathcal{G}}(n.E)e^{-in\omega t}$. The first term is the frozen Green function

$$\hat{G^f}(t,E)=\left[\hat{1}\;E-\hat{\mathcal{H}}_c^t+i\frac{\hat{\Gamma}}{2}\right]^{-1}, \tag{39}$$

corresponding to the frozen Hamiltonian at time t, $\hat{\mathcal{H}}_c^t=\hat{\mathcal{H}}_c(t)$ ($\hat{\Gamma}$ collects the hybridization functions of the reservoirs). The next term is first order in ω. It reads

$$\hat{G^{(1)}}(t,E)=\frac{\hbar}{2}\partial_E\partial_t\hat{G^f}(t,E)+\hat{\mathcal{A}}(t,E), \tag{40}$$

where

$$\hat{\mathcal{A}}=\frac{\hbar}{2}\left(\partial_E\hat{G^f}(t,E)\frac{d\hat{V}}{dt}\hat{G^f}(t,E)-\hat{G^f}(t,E)\frac{d\hat{V}}{dt}\partial_E\hat{G^f}(t,E)\right). \tag{41}$$

The expansion of the Floquet scattering matrix up to the first order in the driving frequency ω cast

$$s_{ij}(E,E_n)=\frac{1}{\tau}\int_0^{\tau}dt\;e^{-in\omega t}[s_{ij}(t,E)+\frac{n\hbar\omega}{2}\partial_E s_{ij}(t,E)+\hbar\omega A_{ij}(t,E)].$$

Here $s_{ij}(t,E)$ is the frozen scattering matrix. The matrix elements $A_{ij}(t,E)$ define a first order correction to the adiabatic scattering matrix. The frozen scattering matrix $s_{ij}(t,E)$ as well as $A_{ij}(t,E)$ do not change significantly on the energy scale $\hbar\omega$ and T and depend on the specific realization of the scatterer. Anyway, it can be shown that, due to the unitarity of the Floquet scattering matrix and of the frozen scattering matrix they satisfy [10]

$$\hbar\omega[\hat{s}^\dagger\hat{A}+\hat{A}^\dagger\hat{s}]=\frac{i\hbar}{2}\left(\frac{\partial\hat{s}^\dagger}{\partial t}\frac{\partial\hat{s}}{\partial E}-\frac{\partial\hat{s}^\dagger}{\partial E}\frac{\partial\hat{s}}{\partial t}\right). \tag{42}$$

Equation (36) defines an explicit relation between $\hat{\mathcal{A}}$ and $\hat{A}$ [26].

Transport coefficients

Substituting the expansions for the Fermi function (37) and for the Green function (38) into Eqs. (32), (33) and (35) and collecting terms up to first order in the affinities $X_1=\frac{\delta\mu}{T}$, $X_2=\frac{\delta T}{T^2}$ and $X_3=\frac{\hbar\omega}{T}$ we obtain:

$$\begin{aligned}
L_{11}&=-\frac{T}{h\mathcal{T}}\int_0^{\mathcal{T}}dt\int_{-\infty}^{+\infty}dE\frac{df}{dE}|\hat{G}^f_{RL}(t,E)|^2\hat{\Gamma}_L\hat{\Gamma}_R\\
L_{12}=L_{21}&=-\frac{T}{h\mathcal{T}}\int_0^{\mathcal{T}}dt\int_{-\infty}^{+\infty}dE(E-\mu)\frac{df}{dE}|\hat{G}^f_{RL}(t,E)|^2\hat{\Gamma}_L\hat{\Gamma}_R\\
L_{13}=-L_{31}&=-\frac{T}{2\pi h}\int_0^{\mathcal{T}}dt\int_{-\infty}^{+\infty}dE\frac{df}{dE}\mathrm{Im}\left\{\left[\hat{G}^f(t,E)\hat{\Gamma}\frac{\partial\hat{G}^{f\dagger}(t,E)}{\partial t}\hat{\Gamma}\right]_{RR}\right\}\\
L_{22}&=-\frac{T}{h\mathcal{T}}\int_0^{\mathcal{T}}dt\int_{-\infty}^{+\infty}dE\,(E-\mu)^2\,\frac{df}{dE}|\hat{G}^f_{RL}(t,E)|^2\hat{\Gamma}_L\hat{\Gamma}_R\\
L_{23}=-L_{32}&=-\frac{T}{2\pi h}\int_0^{\mathcal{T}}dt\int_{-\infty}^{+\infty}dE\,(E-\mu)\,\frac{df}{dE}\mathrm{Im}\left\{\left[\hat{G}^f(t,E)\hat{\Gamma}\frac{\partial\hat{G}^{f\dagger}(t,E)}{\partial t}\hat{\Gamma}\right]_{RR}\right\}\\
L_{33}&=-\frac{T\mathcal{T}}{8\pi^2 h}\int_0^{\mathcal{T}}dt\int_{-\infty}^{+\infty}dE\frac{df}{dE}\mathrm{Re}\left\{\mathrm{Tr}\left[\frac{\partial\hat{G}^f(t,E)}{\partial t}\hat{\Gamma}\frac{\partial\hat{G}^{f\dagger}(t,E)}{\partial t}\hat{\Gamma}\right]\right\}
\end{aligned} \tag{43}$$

Within the scattering matrix formalism the coefficients read

$$\begin{aligned}
L_{11} &= -\frac{T}{h\mathcal{T}}\int_0^{\mathcal{T}} dt \int_{-\infty}^{+\infty} dE \frac{df}{dE}|\hat{s}_{RL}(t,E)|^2 \\
L_{12} = L_{21} &= -\frac{T}{h\mathcal{T}}\int_0^{\mathcal{T}} dt \int_{-\infty}^{+\infty} dE (E-\mu)\, \frac{df}{dE}|\hat{s}_{RL}(t,E)|^2 \\
L_{13} = -L_{31} &= -\frac{T}{2\pi h}\int_0^{\mathcal{T}} dt \int_{-\infty}^{+\infty} dE \frac{df}{dE}\mathrm{Im}\left\{\left[\hat{s}(t,E)\frac{\partial \hat{s}^\dagger(t,E)}{\partial t}\right]_{RR}\right\} \\
L_{22} &= -\frac{T}{h\tau}\int_0^{\mathcal{T}} dt \int_{-\infty}^{+\infty} dE (E-\mu)^2\, \frac{df}{dE}|\hat{s}_{RL}(t,E)|^2 \\
L_{23} = -L_{32} &= -\frac{T}{2\pi h}\int_0^{\mathcal{T}} dt \int_{-\infty}^{+\infty} dE (E-\mu)\, \frac{df}{dE}\mathrm{Im}\left\{\left[\hat{s}(t,E)\frac{\partial \hat{s}^\dagger(t,E)}{\partial t}\right]_{RR}\right\} \\
L_{33} &= -\frac{T\mathcal{T}}{8\pi^2 h}\int_0^{\mathcal{T}} dt \int_{-\infty}^{+\infty} dE \frac{df}{dE}\mathrm{Tr}\left[\frac{\partial \hat{s}(t,E)}{\partial t}\frac{\partial \hat{s}^\dagger(t,E)}{\partial t}\right].
\end{aligned} \tag{44}$$

The matrices $\hat{\mathcal{A}}$ in the Green-function language, and $\hat{A}$ in the scattering matrix version, in principle seem to contribute to the coefficient L_{33}. In particular, they appear in an integrand of the form

$$\sum_{ij} 2\mathrm{Im}\left\{A_{ij}(t,E)\frac{\partial s^*_{ij}(t,E)}{\partial t}\right\}. \tag{45}$$

However, as shown in Ref. [22], due to the unitary condition of the frozen scattering matrix $\hat{s}\hat{s}^\dagger = 1$ and the property (42) such term vanishes. In fact, it can be also written as

$$\begin{aligned}
&2\mathrm{Im}\left\{\mathrm{Tr}\left[\partial_t \hat{s}^\dagger \hat{A}\right]\right\} = -i\mathrm{Tr}\left[\partial_t \hat{s}^\dagger \hat{A} - \hat{A}^\dagger \partial_t \hat{s}\right] = -i\mathrm{Tr}\left[\left(\hat{s}^\dagger \hat{A} + \hat{A}^\dagger \hat{s}\right)\partial_t \hat{s}^\dagger \hat{s}\right] \\
&= \frac{1}{2\omega}\mathrm{Tr}\left[\left(\partial_t \hat{s}^\dagger \partial_E \hat{s} - \hat{s}^\dagger \partial_E \hat{s}\partial_t \hat{s}^\dagger \hat{s}\right)\partial_t \hat{s}^\dagger \hat{s}\right] = 0.
\end{aligned} \tag{46}$$

3. EFFICIENCY

Thermodynamic bounds

In this section we show that the second principle of the thermodynamics imposes upper bounds for the efficiency of the devices.

We start with the motor, in which case an appropriate measure of the efficiency η^{mot} is the ratio between the net power delivered by the electrons against the *ac* forces and the net power delivered by the battery with a voltage difference $\delta\mu/e$ to keep a net flow of outgoing current $\dot{N}$ from the highest chemical potential reservoir. In the case of the generator, the relevant ratio to compute the efficiency η^{gen} is the inverse one. Hence, recalling that we consider as positive the current outgoing the leads and thus incoming into the reservoir and having $\mu_L = \mu_R + \delta\mu$, $T_L = T_R = T$

$$\eta^{\mathrm{mot}} = \frac{1}{\eta^{\mathrm{gen}}} = \frac{-\overline{\dot{W}}}{\overline{\dot{N}}_R \delta\mu/e}. \tag{47}$$

Since $\overline{\dot{S}} = \frac{\overline{\dot{Q}}_L}{T_L} + \frac{\overline{\dot{Q}}_R}{T_R}$, combining $\overline{\dot{Q}}_\alpha = \overline{\dot{E}}_\alpha - \mu_\alpha \overline{\dot{N}}_\alpha$ and Eq. (5), we have

$$\overline{\dot{W}} = T\overline{\dot{S}} - \frac{\delta\mu}{e}\overline{\dot{N}}_R. \tag{48}$$

Substituting Eq. (48) into Eq. (47) we have

$$\eta^{\mathrm{mot}} = \frac{1}{\eta^{\mathrm{gen}}} = 1 - \frac{T\overline{\dot{S}}}{\overline{\dot{N}}_R \delta\mu/e}. \tag{49}$$

Hence, the second principle of thermodynamics implies $\overline{\dot{S}} > 0$, which imposes the bound $\eta^{\text{mot/gen}} \leq 1$.

Similarly in the case of an heat pump, an appropriate measure of the efficiency η^{he} is the ratio between the net power delivered by the electrons against the *ac* forces and the heat leaving the hot reservoir Q^{hot}. In the case of a heat pump, the relevant ratio to compute the efficiency η^{hp} is the inverse one. Hence, recalling that we consider as positive the current outgoing the leads and thus incoming into the reservoir and having the reservoir L as the hot one, $T_R = T_L - \delta T$ and $\mu_L = \mu_R = \mu$

$$\eta^{\text{he}} = \frac{1}{\eta^{\text{hp}}} = \frac{\overline{\dot{W}}}{\overline{\dot{Q}}_L}. \tag{50}$$

Since $\overline{\dot{S}} = \frac{\overline{\dot{Q}}_L}{T_L} + \frac{\overline{\dot{Q}}_R}{T_R}$, combining $\overline{\dot{Q}}_\alpha = \overline{\dot{E}}_\alpha - \mu_\alpha \overline{\dot{N}}_\alpha$ and Eq. (5), we have

$$\eta_c \overline{\dot{Q}}_L = -T_R \overline{\dot{S}} + \overline{\dot{W}}. \tag{51}$$

where $\eta_c = \delta T / T_L$ is the Carnot efficiency for an heat engine. Substituting Eq. (51) into Eq. (50) we have

$$\eta^{\text{he}} = \frac{1}{\eta^{\text{hp}}} = \eta_c \big[1 - \frac{T_R \overline{\dot{S}}}{T_R \overline{\dot{S}} - \overline{\dot{W}}}\big]. \tag{52}$$

In this case, the second principle imposes the bound of the Carnot efficiency for the heat engine and the heat pump, $\eta^{\text{he/hp}} \leq \eta_c^{\text{he/hp}}$.

Maximum efficiency

We focus on the linear response regime and $B = 0$, in which case $L_{13} = -L_{31}$ while $L_{23} = -L_{32}$. We also recall that the second principle imposes that the diagonal coefficients are all positive, as mentioned in the main text.

Efficiency: motor and heat engine

We calculate the maximum efficiency in the case of motors or heat engines when $L_{13}\delta\mu/T > 0$ and $L_{23}\delta T/T^2 > 0$. As defined in the main text it reads

$$\eta^{\text{mot/he}} = -\frac{X_3 J_3}{X_i J_i}, \tag{53}$$

with $i = 1$ for motors and $i = 2$ in the case of heat engines.

Assuming X_3 constant, we find that the value of X_1 (in the motor mode) or X_2 (in the heat engine mode) that maximizes the efficiency is

$$X_i = \frac{L_{ii}L_{33} + \sqrt{L_{ii}L_{33}\det(\hat{L})}}{L_{ii}L_{i3}} X_3. \tag{54}$$

Substituting Eq. (54) into Eq. (53) we have Eqs. (13-16).

Alternatively, we can assume that X_1 (motor mode) or X_2 (heat engine mode) are fixed and find which value of X_3 yields a maximum in the efficiency. In this case it is found

$$X_3 = \frac{-L_{ii}L_{33} + \sqrt{L_{ii}L_{33}\det(\hat{L})}}{L_{33}L_{i3}} X_i, \tag{55}$$

which when substituting into Eq. (53) also leads to Eqs. (13-16). Hence, the latter expressions for the maximum efficiency correspond to fixing any of the two relevant affinities.

Efficiency: generator and heat pump

We can proceed in a similar way when the device pumps charge against a voltage drop (generator mode) or heat against a thermal gradient (heat pumping mode). In this case $L_{13}\delta\mu/T < 0$ and $L_{23}\delta T/T^2 < 0$. The efficiency is the inverse of the one defined for motors and heat engines

$$\eta^{\mathrm{gen/hp}} = -\frac{X_i J_i}{X_3 J_3}, \tag{56}$$

with $i = 1$ for generators and $i = 2$ in the case of heat pump.

The maximum efficiency at a given driving frequency, *i.e.* with constant X_3 corresponds to values of the bias voltage or the thermal gradient (X_1 or X_2) given by

$$X_i = \frac{L_{ii}L_{33} - \sqrt{L_{ii}L_{33}\det(\hat{L})}}{L_{ii}L_{i3}} X_3, \tag{57}$$

which leads to Eqs. (13-16).

As before, we can also choose to keep X_1 (for the generator) or X_2 for the heat pump fixed and extract the value of X_3 corresponding to the maximum efficiency. This yields

$$X_3 = -\frac{L_{ii}L_{33} + \sqrt{L_{ii}L_{33}\det(\hat{L})}}{L_{33}L_{i3}} X_i. \tag{58}$$

When substituting into (56) we get again Eqs. (13-16).